Tagging single muons and other long-flying relativistic charged particles by ultra-fast timing in air Cherenkov telescopes

R. Mirzoyan [a,1], D. Sobczynska [b], E. Lorenz [a], M. Teshima [a]

[a] *Max-Planck-Institut für Physik, Föhringer Ring 6, D-80805 München, Germany*

[b] *University of Łódź, PL-90236 Lodz, Poland*

Abstract

Atmospheric air Cherenkov telescopes are successfully used for ground-based, very high-energy (VHE) γ ray astronomy. Triggers from the so-called single muon and other long-flying relativistic charged particle events are an unwanted background for the Cherenkov telescope. Because of low rate at $\sim TeV$ energies the muon background is unimportant. It is much more intense for telescopes with high photon sensitivity and low energy threshold. Below a few hundred GeV energy, the so-called muon background becomes so intense, that it can deteriorate the sensitivity of telescopes (the so-called "*muon-wall*" problem). From general considerations it can be anticipated that the signature of these particles should be a light pulse with a narrow time structure. In fact, simulations show that the pulses from muons have a very narrow time profile that is well below the time resolutions of nearly all currently operating telescopes. In this report we elaborate on the time profile of Cherenkov light from the so-called single muons and show that a telescope with ultra-fast time response can open a new dimension allowing one to tag and to reject those events.

Key words: Gamma-ray Astronomy, Imaging atmospheric air Cherenkov

telescopes, Single muons, Trigger from muons

PACS: 95.55.Ka, 95.55.Vj, 95.75.-z, 95.55.Mn, 95.85.Pw, 95.85.Ry

References

[1] T.C. Weekes et al., Observation of TeV gamma rays from the Crab nebula using the atmospheric Cherenkov imaging technique, Astrophys. J. **342** (1989) 379–395.

[2] A.M. Hillas, *Proc. 19th ICRC, La Jolla*, **3** (1985) 445–449.

[3] T.C. Weekes, VERITAS Status Report, *Proc. Towards a Network of Atmospheric Cherenkov Detectors-VII conf.*, ed. B. Degrange, Ecole Polytechnique, Palaiseau, France, 27-29 April 2005, in press.

[4] M. Mori, CANGAROO Status Report, *Proc. Towards a Network of Atmospheric Cherenkov Detectors-VII conf.*, ed. B. Degrange, Ecole Polytechnique, Palaiseau, France, 27-29 April 2005, in press.

[5] M. Mariotti, MAGIC Status Report, *Proc. Towards a Network of Atmospheric Cherenkov Detectors-VII conf.*, ed. B. Degrange, Ecole Polytechnique, Palaiseau, France, 27-29 April 2005, in press.

[6] W. Hofmann, H.E.S.S. Status Report, *Proc. Towards a Network of Atmospheric Cherenkov Detectors-VII conf.*, ed. B. Degrange, Ecole Polytechnique, Palaiseau, France, 27-29 April 2005, in press.

[7] G. Vacanti et al., Muon ring images with an atmospheric Cherenkov telescope, Astropart. Phys. **2** (1994) 1–11.

---

[1] Corresponding author

[8] V.R. Chitnis, P.N. Bhat, Simulation Studies on Arrival Time Distributions of Cherenkov Photons in Extensive Air Showers, Astropart. Phys. **12** (1999) 45–64.

[9] H. Cabot et al., Measurable difference in Cherenkov light between gamma and hadron induced EAS, Astropart. Phys. **9** (1998) 269–276.

[10] J. Knapp, D. Heck, *EAS Simulation with CORSIKA: A Users Manual* (2004).

[11] H. Bartko, F. Goebel, R. Mirzoyan et al., Tests of a prototype multiplexed fiber-optic ultra-fast FADC data acquisition system for the MAGIC telescope, Nucl. Instr. and Meth. A **548** (2005) 464–486.

[12] D. Smith, Review of the "Solar Array" Cherenkov telescopes, *Proc. Towards a Network of Atmospheric Cherenkov Detectors-VII conf.*, ed. B. Degrange, Ecole Polytechnique, Palaiseau, France, 27-29 April 2005, in press.

1   Introduction

The window of ground-based γ astronomy was opened in 1989 by the observation of a strong signal from the first TeV source, the Crab Nebula, by the Whipple collaboration [1]. A major breakthrough in the technique was the image parameterization suggested by Hillas in 1985 [2]. This parameterization allowed the efficient separation of rare γ ray events from the orders of magnitude more intense background from the charged cosmic rays (CR). Since then, this new field of astronomy has progressed very rapidly and all new source discoveries have been made by means of this new type of telescopes, the so-called imaging air Cherenkov telescopes (IACT). Currently, a new generation of very large IACTs [3], [4], [5], [6] have either started to operate or are in the final phase of completion. It is hoped that the energy window from a few tens of

GeV ($(30-200)GeV$, depending on the instrument) up to the multi-TeV, can thus be exploited. Already discussions and planning are underway for future IACTs with a threshold close to $(5-10)GeV$. In order to achieve a very low energy threshold, it is necessary to build telescopes with a very large reflector area. With lower energy, the background caused by triggers from hadron showers decreases progressively, while other backgrounds become more dominant. One such backgrounds, namely air showers induced by cosmic electrons, cannot be strongly suppressed with current tools (except by using a telescope's angular resolution), because the electrons produce electromagnetic showers, in practice, indistinguishable from those of the γ. Below $(10-30)GeV$, depending on telescope location and observation direction, the earth's magnetic field deflects cosmic electrons out of the detection volume in the atmosphere. Another very likely irreducible background is caused by hadron interactions transferring a large fraction of their energy to a π°, which subsequently decays into 2γ and thus generates a dominantly electromagnetic shower. One of the main backgrounds is caused by Cherenkov light flashes from single, long-flying relativistic charged particles high up in the atmosphere. This background is called, in the community, the muon background, but there can also be contributions from the muon parents, relativistic charged pions, kaons or protons. There may also be contributions from a fraction of single, straight, long-flying electrons that can survive a few radiation lengths without bremsstrahlung losses. For clarifying the question about the particle types producing triggers in a Cherenkov telescope we performed special Monte Carlo simulations of hadron showers. In these simulations we followed cases in which almost the entire light came from either a) muons or from b) pions, kaons and protons. It turned out that the channel a) is the dominant one and that it is, at least by an order of magnitude, more frequent compared to channel b). For conve-

nience further in the text we will use the name muon (μ) background for all the above-discussed cases. The μ (π) can have a large angular deviation from their parent hadron shower's axis and thus can appear unaccompanied in the relatively small field of view of a Cherenkov telescope. That shall be one of the reasons why they are called "single μ events". It is interesting to note that a wide field of view telescope can be helpful in rejecting the μ (hadronic) background: often together with the μ it will measure also their parent particles (or showers).

2   The image shapes produced by muons

An air Cherenkov telescope, depending on its photon sensitivity (light collection area and efficiency), can trigger on μ in a wide range of impact parameters. For example, a very sensitive $17m$ diameter telescope, comprising a mirror area of $\sim 240m^2$, would trigger on μ with energy $\geq 30GeV$ anywhere up to the so-called hump in the lateral distribution of Cherenkov light at $\sim 120m$ (see Fig.1). The shape of a μ image depends on its energy and impact parameter and on the incident angle (for details see [7]). For any selected azimuth direction and for a short height interval a relativistic μ emits a parallel beam of light along the Cherenkov light cone opening angle $\theta_{Cher.}$. For simplicity, let us consider a μ that hits the telescope on-axis. Light from the μ from the given azimuth will be focused by the telescope optic into a spot that is at an angular distance of $\theta_{Cher.}$ from the imaging camera center. Thus the emitted light from all the azimuth angles of the cone will be focused into a ring-shaped image of radius $\theta_{Cher.}$ in the focal plane. The thickness of the ring is largely due to variations in the Cherenkov light emission angle along the μ track.

Close to the Cherenkov light emission threshold (that is, for example, $5GeV$ for μ at $2200m$ a.s.l.) a μ can produce thick rings of smaller radii than the $\theta_{Cher.}$. A μ that hits anywhere in the reflector area of a telescope will produce a circular image of varying charge density along the circle and only in the case of an on-axis hit will it produce a "constant" charge density along the ring. The maximum height for a μ above the reflector area in which it still can produce a ring image is defined by the reflector's diameter and by the Cherenkov angle for the location height. For example, a $17m$ diameter IACT can see the light from on-axis μ below height of $\sim 400m$. With the increase of the impact parameter up to $\sim 30m$, a μ will produce image shapes that one can still recognize as an arc (see Fig.2). Beyond that, until the impact parameter of $\sim (60-70)m$, the arc image shape will shrink in length, essentially imitating short straight lines. The scarce photon statistics of the image and the usually relatively coarse pixel size of the imaging cameras make it even more difficult to reveal any hint of slight curvature in a short quasi-straight line. The images of μ shrink to essentially small spots (of high-charge concentration) for impact parameters $\geq 80m$. The above-mentioned quasi-straight line images produced by μ can easily mimic the expected image shapes of γ. One can estimate that for the impact parameters range $\sim (30-60)m$, a telescope of $240m^2$ reflector area will collect ~ 1500 photons from a μ (see Fig.1). Assuming an average photon to photo electron ($ph.e.$) conversion efficiency of $\sim 10\%$ this will correspond to a $\sim 150 ph.e.$ signal for those μ events. That intensity is comparable to the image intensity produced by γ showers near the threshold energy. This is possible because one can measure as many photons from a single long-flying μ in the field of view of a telescope as from many e^+e^- of short track lengths together in an air shower. In addition, because of the isotropic flux, some of those μ events will have the expected orientation

of the γ images and thus can pass the signal selection criteria. Those misclassified events can be numerous and thus can deteriorate the sensitivity of a telescope to genuine γ. Also stereoscopic telescope configurations, providing high photon sensitivity, will trigger on μ in a wide range of impact parameters. A typical μ will produce arcs of different lengths in different telescopes, so one can tag it. Frequently a stereoscopic telescope system will measure μ events seen only by two telescopes (here we assume a trigger configuration of "$any \geq 2 \ telescopes \ out \ of \ N$" where N is the total number of telescopes). Part of these μ, especially those coming from large impact parameters, can mimic γ. Of course, compared to a single telescope the rate of such events will be much lower. If the photon sensitivity of stereo telescopes, set into hardware coincidence, is not very high then only one of the telescopes, the closest one to the μ impact point can produce trigger. Thus such a system will strongly suppress that annoying background but only at the expense of relatively high energy threshold. There is a first order correlation between the reflector diameter and the track length of a particle seen in Cherenkov light. At large impact distances a $10m$ diameter dish collects light from approximately one radiation length of the track of an ultra-relativistic particle. It is interesting to note that μ images from large impact parameters become elongated in the axial direction (see the image shape for $120m$ impact distance on Fig.2). This reflects the variation of the refraction index and, correspondingly, of the Cherenkov light emission angle in the air when a μ traverses long distance in height, remaining in the telescope's field of view. In this article we want to report on ultra-fast timing features of μ events that can open a new dimension in Cherenkov technique allowing one to tag and to reject them. As will be shown in the Monte Carlo (MC) section the characteristic time spreads are typically in the range of $(100 - 200)ps$ for μ images, $(2 - 3)ns$ for γ and $(3 - 5)ns$

(with significant tails) for hadrons. In the following we will present detailed MC studies, discuss the possible performance and outline how a best-possible system for μ suppression should look.

3 Triggers from muons: a closer look

3.1 Expected ultra-short pulse in time

The arrival time distribution of Cherenkov photons from extensive air showers has been extensively studied (see, for example, [8], [9]). One may assume that measured photon arrival time structures from an air shower of a given impact parameter and of a given incident angle are due to

- the shower's transverse and longitudinal size seen by the telescope, the longitudinal size being the dominant effect
- shower particle velocity differences from the speed of light along the shower's longitudinal development
- energy-dependent multiple-scattering angle of shower particles along the shower height
- angular deviation of produced particles from the primary direction

The elastic scattering effects in the earth's magnetic field may also contribute into the time structure. Unlike air showers a single μ has no transverse size. Also the last point in the above list cannot contribute into the time structure of light pulse from a μ. The light from a μ has a time structure only because of the other criteria above. Calculations show that light emitted at a height of $35km$ will arrive $\sim 6ns$ later than the light emitted immediately above the

ground level due to the higher speed of a relativistic μ compared to that of light in the atmosphere. On the other hand, a telescope, because of it's limited field of view can only observe a small part of the track of a μ (as outlined in the previous chapter) that will, correspondingly, produce a very short flash. To quantify the effect of the other influences we have performed Monte Carlo simulations.

3.2   Monte Carlo simulations

We used the version 6.023 of the CORSIKA code in our simulations [10]. Our statistics is based on 7.5×10^5 simulated proton showers in the energy range $(0.04 - 30)TeV$ following a power-law of index -2.75. The impact parameter range for the protons was up to $300m$. They were simulated from a zenith angle of $20°$ and within the cone opening angle $2.5°$. All μ produced were tracked. Along with protons 35000 γ showers were simulated in the energy range $(0.01 - 30)TeV$ following a power-law of index -2.6, impact parameter range up to $300m$ and the zenith angle of $20°$. Also 4×10^5 μ were simulated in the energy range $(10 - 100)GeV$, following a power-law of index -2.69 and impact parameter range up to $200m$, within $1.2°$ around the observation direction. These μ were injected into the atmosphere at $100g/cm^2$ (corresponding to height in the atmosphere of $\sim 17km$). Depending on the problem under study we used different samples of the simulated events. In addition, we simulated 5×10^5 proton showers of fixed energies 50, 100, 300 and 500 GeV impinging from the zenith angle $0°$. This sample was used to produce Fig.3a in which we show the average number of produced μ versus the altitude in the atmosphere (for every $1km$ height interval) and Fig.3b in which we show the

9

same but only for μ that are above the Cherenkov light production threshold for the given height. The areas under the corresponding histograms on Fig.3 are the average number of μ produced in a shower of a given energy. One can see that the maxima of μ production for different primary energies are around the height range of $10 - 12km$. The 50, 100, 300 and 500 GeV proton samples were used to produce Fig.4 which shows the probability of angular deviation of μ from the primary direction. The angle is measured in the last part of the μ trajectory just before it hits the observation level. In Fig.4a one can see the angular deviation for all μ and in Fig.4b only for those that are above the light production threshold (the area under the distributions are normalized to 1). While at high energies the angular distribution can be characterized by a $\sim 1°$, it is wider (with a tail extending up to $(4-6)°$) for lower energies (see the curve produced by $50GeV$ protons). The qualitative picture is clear: at low energies the secondary particles are at wider angles to the primary direction (read: the probability is high that a μ can appear as a "single" particle in the limited field of view of the imaging camera). By switching the earth's magnetic field on and off in Monte Carlo simulations, we found that it does not influence the width and the shape of the angular deviation of the μ. Also, the estimates of the multiple scattering effect of μ provide lower value of the deviation angle from the primary direction than the results of the simulations show. The reason for this difference can be due to the known non-Gaussian larger tails in the real scattering process. Fig.5 shows the characteristic photon arrival time profiles for μ, γ and hadrons at the observation level of $2200m$ a.s.l.. One can see that the time structure of light flashes from μ is $(100-200)ps$ wide. There is a small tail in the distribution where μ produce somewhat longer pulses but, as one can see, those happen rarely. Typically, the γ flashes at low energies are $(2-2.5)ns$ wide while the majority of protons produce flashes of $(2-6)ns$

wide with a tail extending beyond $10ns$. Also, one can see in Fig.5 that the photon arrival time distribution from γ showers has nearly Gaussian shape, while the same from protons is significantly asymmetric.

4 Muon tagging by a telescope

The measured signal from a telescope is a convolution of the incident light time profile with the response functions of a) the reflector, b) the light sensors and c) the readout system. When identifying μ, because of their ultra-fast flashes (see Fig.5), one would search for pulses close to the instrumental response to instantaneous charge injection. Anything larger than that will be due to other reason than the detection of a μ. In the ideal case, the instrumental response function must be ultra-fast in order not to smear the time signature of μ and to provide discrimination power. Below we list the main parameters that determine the instrumental time response of a telescope:

- design of the reflector
- speed of the focal plane light sensors
- speed of the data acquisition system

Let us discuss the above listed factors.

Design of the reflector: it is well known that a parabolic reflector has no time dispersion at the focal plane for a parallel beam of light arriving on-axis. For an off-axis parallel beam of light inclined to $1°$, for a parabola of $F/1$ optics, one will obtain a time dispersion of slightly less than $140ps$. Calculations show that for larger angles, up to a few degrees, that value increases only marginally. Usually, the field of view of relatively fast design parabolic reflectors ($F/D \sim$

1), which can provide optical resolutions of $\sim (0.05 - 0.1)^\circ$ acceptable for air Cherenkov telescopes, is limited to $(1 - 1.5)^\circ$ in radius, so the time dilution caused by the above mentioned effect will be small. One may conclude that a reflector of parabolic design is appropriate for ultra-fast timing purposes (see, for example, [5]). There can be other factors which deteriorate the timing profile but usually all of these will have minor contributions. There can be contributions because of the

- tessellated design of the reflector; the shape of individual mirrors deviate at the edges from the perfect parabola. This effect shall be below $100ps$, even in the case of fast optics and of relatively large mirror tiles of $\sim 1m$ size.
- differences in the fixation of the mirror tiles on the reflector that could result in deviation from the parabolic shape. One may assume that this effect can be relatively easy controlled and that the deviations can be kept below $2cm$. That will result in time smearing of $\leq 120ps$.
- use of light concentrators in front of the sensors in the camera to minimize the light losses. Light can hit the sensors directly or via single or double reflections from the concentrator. Path differences of $\leq (2-3)cm$ will result in time smearing of $\leq 100ps$.

Several other reflector designs exist that, unfortunately, always expand the time profile of input light. The commonly used Davies-Cotton design widens the input pulse, even for the on-axis light flash, to for example, $(0.3ns/m) \times F(m)$ for $F/D = 1.2$.

Ultra-fast light sensors: until now the classic photo-multiplier tubes (PMT) have been the only light sensors used in the focal plane imaging cameras of Cherenkov telescopes. Usually their response is in the range of $(2-3)ns$ but very fast tubes also exist. For example, in the MAGIC telescope project,

6-dynode, hemi-spherical bialkali 1" PMTs from Electron Tubes (ET9116A) are used. They provide rise and fall times of 0.6ns and 0.7ns, respectively, and a pulse width of $(1.0 - 1.2)ns$. The measured transit time spread (TTS) is $\leq 300ps$. So a δ-function-like light flash at the input of these PMTs will produce an ultra-short pulse with the above-mentioned parameters.

Ultra-fast readout system: in order to provide any meaningful pulse shape reconstruction, assuming a Gaussian-shaped input pulse profile, one needs at least $3 - 4$ sampling points. By using an ultra-fast readout system of $\geq 2Gsample/s$ one can reconstruct the very fast pulse shapes from, for example, above mentioned ultra-fast PMTs (see, for example, [11]).

5 Discussion: μ suppression by ultra-fast timing

From the discussion above one may conclude that it is currently possible to design a telescope that can produce ultra-short signal pulses of $\sim 1.5ns$, as a response to δ-function like light flashes (as for example, from μ). The μ flashes will generate output pulses that should be only marginally wider than the instrumental response function of a telescope. This can be used as a criterion to distinguish them from γ and proton air showers. Although Cherenkov flashes produced by γ showers are significantly shorter and have smoother time profile compared to those produced by hadrons (see below), still they have $\sim (2 - 3)ns$ time structure that is significantly wider than that of μ. We have also calculated the root mean squared ($r.m.s.$) value of the arrival time distribution for all γ, proton and μ events measured by a $17m$ telescope with an ultra-fast response function. In addition to the above-mentioned parameters for the PMT, we simulated output pulses with realistic transit time spread (TTS)

13

of $\sigma = 300ps$. We have used a trigger condition *any 4 next neighbor pixels above a given threshold* in our simulations. The corresponding distributions are shown on Fig.6. One can see a good separation of the μ events from γ. In fact, there are no γ events with $r.m.s. \leq 0.7ns$ or with $r.m.s. \geq 3.5ns$. All events with $r.m.s.$ time spread $\leq 0.7ns$ are μ. It is also interesting to study the dependence of the $r.m.s.$ time width on the image $SIZE$ (measured as the sum of detected $ph.e.$). The corresponding distributions are shown in Fig.7a. The $r.m.s.$ distributions of the γ and of the μ overlap in small $SIZE$ region. When applying a simple set of loose supercuts based on the *length, width, distance* and the *alpha* parameters for γ/hadron separation, the situation is almost the same (see Fig.7b). In contrast, the new cut on the $r.m.s.$ time spread can strongly suppress the unwanted μ background.

5.1 *Gamma telescopes based on solar arrays*

Note please that the above mentioned is equally true for imaging air Cherenkov telescopes and for solar array type γ telescopes. The latter telescopes (for a recent review see [12]) shall also experience μ background. On the other hand, as a rule, those instruments have an ultra-fast response and a readout that could help to tag μ. Application of the proposed new technique can improve the sensitivity of the solar array-type γ telescopes.

5.2 *Stereoscopic telescope systems and wide field of view telescopes*

The imaging stereoscopic telescope systems, providing high photon sensitivity and low threshold, will effectively trigger on μ. Due to the multiple views and

produced different arc lengths and shapes in different telescopes, as a rule one can tag the μ. Still some part of μ, especially those from large impact parameters, can survive the image cuts and mimic γ.

A wide field of view telescope could offer another remedy to tag the μ: frequently one can detect also their parent showers (or particles) that will help the identification. It seems that also in this case part of the μ could be misclassified, especially those detected near the camera edges.

An ultra-fast telescope design will help both in the case of the stereo and wide field of view telescopes allowing one to effectively tag the misclassified μ.

6 Conclusions

We have shown that light pulses from single, long-flying relativistic charged particles have an ultra-narrow time structure. The differences in pulses generated by the μ, γ and hadron events are large enough so that one can efficiently tag and suppress the μ events. The new method suggested here opens a new dimension for the solution of the so-called "μ-wall" problem: ultra-fast telescopes, both of imaging and non-imaging types, including the solar array types, can provide very efficient μ suppression.

The new method can directly increase the sensitivity of the ground-based γ ray telescopes.
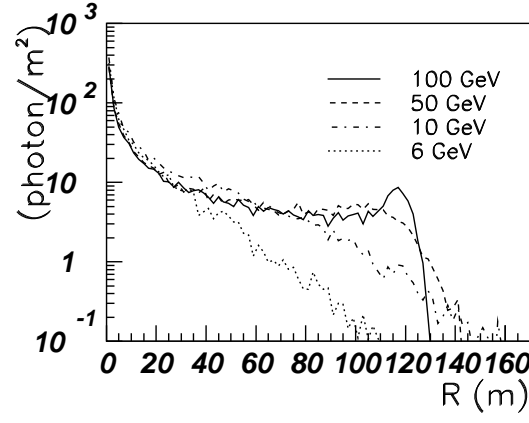
Acknowledgements

Fig. 1. *Simulated lateral distribution of Cherenkov light density on the 2200 m a.s.l. from a 6, 10, 30 and 100 GeV μ, injected at a height of 17 km in the atmosphere.*
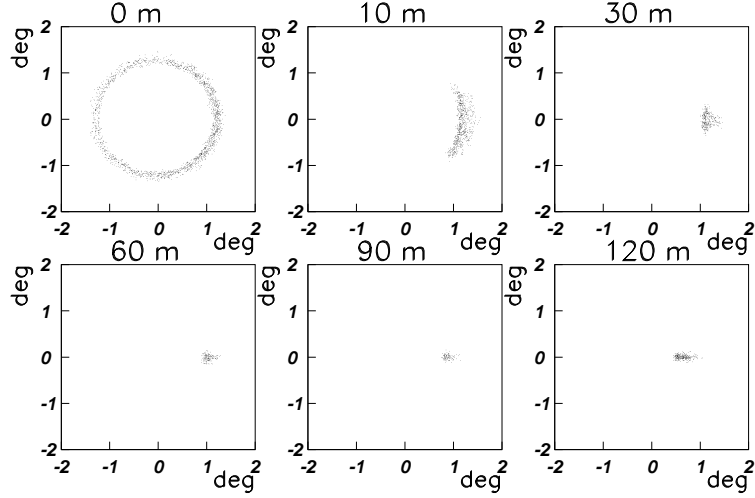

Fig. 2. *Induced by μ arc-shape images in the focal plane of a telescope as function of impact parameter. The images include optical aberrations and are simulated for a 17m diameter telescope.*
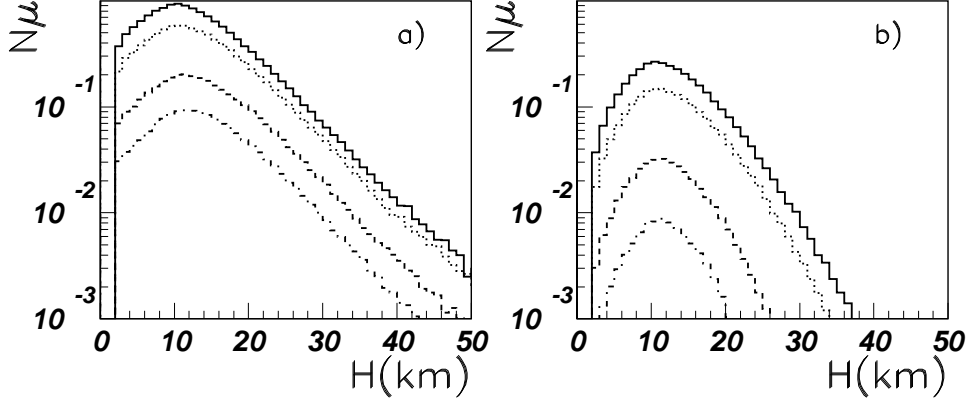
Fig. 3. *Number of μ in air showers versus the production height in the atmosphere. The distributions for proton energies of 50, 100, 300 and 500 GeV are shown, from the bottom upwards: a) all μ; b) only μ that are above the Cherenkov threshold for the given height.*
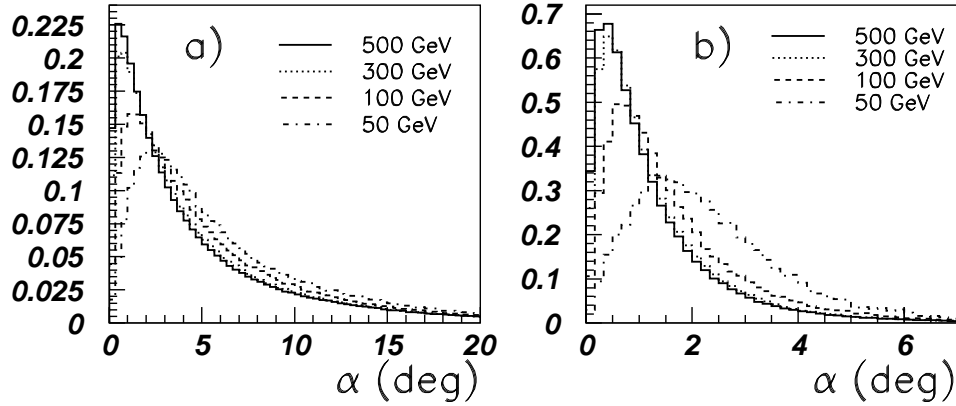

Fig. 4. *Probability of angular deviation of μ (in fact, the angle of μ intersection with the observation level) from the primary proton direction, shown for primary energies of 50, 100, 300 and 500 GeV: a) all μ; b) only μ above the Cherenkov threshold at corresponding heights. The areas under the distributions are normalized to 1.*
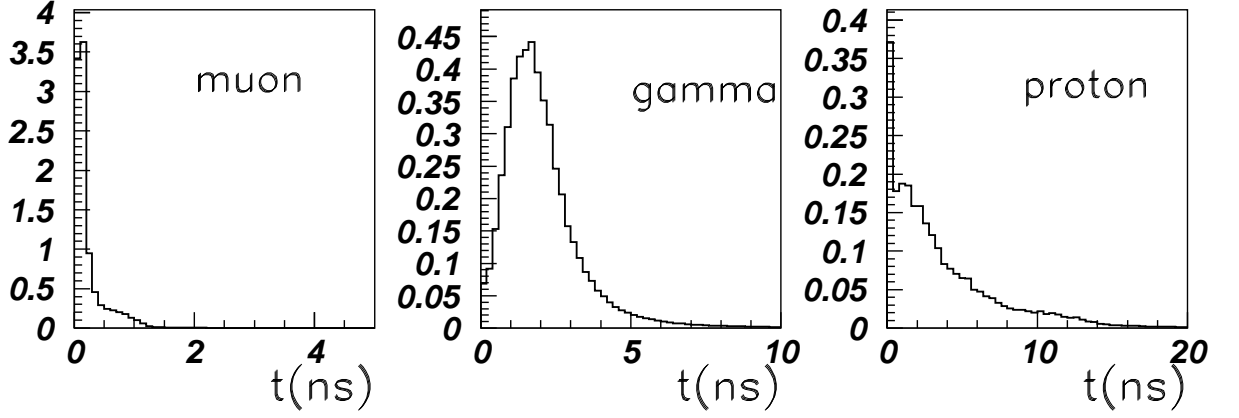
Fig. 5. *Photon arrival time distributions for μ, γ and protons. The distribution for μ is essentially below $(100-200)ps$. Photons from a γ shower (from a weighted spectrum) arrive within $(2-2.5)ns$ while photons from a proton shower arrive essentially in $(2-6)ns$ with a tail extending beyond $10ns$.*
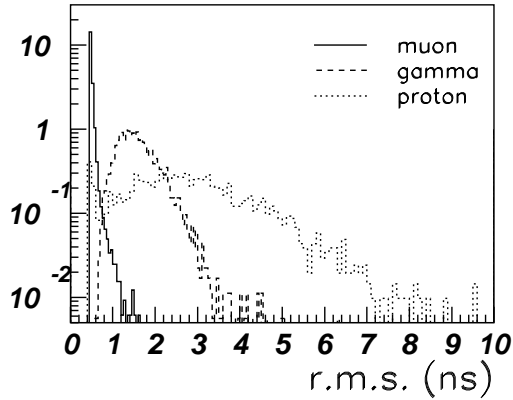

Fig. 6. *Distributions of the r.m.s. value of the arrival time distribution for all γ, proton and μ events measured by a 17m ultra-fast telescope. The events with r.m.s. $\leq 0.7ns$ are of μ origin.*
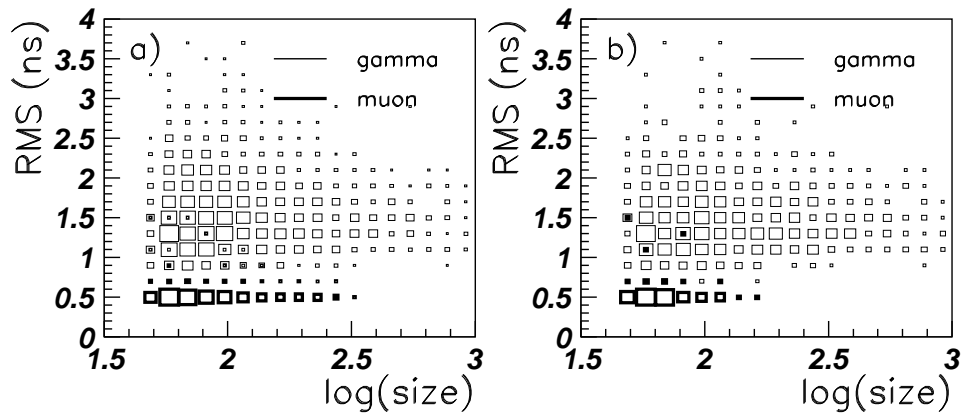
Fig. 7. *Dependence of the r.m.s. time spread of the γ and μ images on the parameter SIZE (sum of registered ph.e.). b) r.m.s. dependence on SIZE after application of simple set of supercuts.*